DE GRUYTER High Temp. Mater. Proc. 2019; 38: 151–157

Bartek Wierzba*, Wojciech J. Nowak and Daria Serafin

The Sequence of the Phase Growth during Diffusion in Ti-Based Systems

https://doi.org/10.1515/htmp-2018-0010
Received January 23, 2018; accepted May 22, 2018

Abstract: The interdiffusion in Ti-based alloys was studied. It was shown that during diffusion at 1,123 K formation of four intermetallic phases occurs. The diffusion paths for six different diffusion couples were determined. Moreover, the entropy production was calculated – the approximation used for determination of the sequence of intermetallic phase formation. In theoretical analysis, the intrinsic diffusion coefficients were determined from the modified Wagner method.

Keywords: diffusion, alloys, titanium compounds, phase equilibria

Introduction

Most of the construction materials are multicomponent and consist of several grains and phases. Their macroscopic properties and reliability highly depend on the microstructure and its evolution in time [1, 2]. Knowledge about high temperature diffusion is essential for better understanding of mechanical properties. The main kinetic parameter describing diffusion in multicomponent system is the intrinsic diffusion coefficient. In binary systems, the Boltzmann–Matano (B-M) analysis [3] can be used for determination of this parameter [4]. The generalization of the B–M analysis in single phase system can be found in our previous papers [5, 6]. However, the determination of the intrinsic diffusion coefficient in multiphase systems is not a trivial task. In binary system, the Wagner method can be used [7]. In ternary and higher system there is lack of such approximations.

The intrinsic diffusion coefficients are very important parameters in computer simulations. For example the phase-field model allows for approximation of solidification [8] process and solid-state phase transformations [9]. Phase-field models are applied for simulating grain growth [10], dislocation dynamics [11–13], crack propagation [14, 15], electromigration [16], solid-state sintering [17–19] and vesicle membranes in biological applications [20, 21].

On the other hand, the knowledge of kinetic parameters allows for extending old problem of phase competition. In binary alloys the problem is usually solved based on the steady-state approximation – analysis of the difference in diffusion coefficients in phases [22]. In ternary and higher systems the analysis of diffusion coefficients is not enough. The entropy production can be calculated – the baricentric average of the fluxes in each phase [23].

In the general case, the diffusion effects in ternary system can be graphically represented in the concentration triangle (precisely in the isothermal section of the equilibrium phase diagram) as a diffusion path. The diffusion path can go across single and two-phase regions in the ternary diagram. In two-phase region, the direction of the diffusion path with respect to tie lines is critical. When the diffusion path enters the two-phase field at the ends of the same tie line, the two-phase zone does not grow. In the spatial region, the interphase boundary between the two phases at the equilibrium (of the compositions indicated by the tie line ends) occurs. When the diffusion path crosses the tie lines, the two-phase zone can grow. The points of the intersection of the diffusion path with the phase boundaries in the phase diagram serve as a basis to identify the sequential single and two-phase layers present in the diffusion zone.

In this paper, the interdiffusion in Ti-CuNi diffusion couples is discussed – six different diffusion couples were prepared, mainly Ti-Ni10Cu90, Ti-Ni30Cu70, Ti-Ni40Cu60, Ti-Ni60Cu40, Ti-Ni70Cu30 and Ti-Ni90Cu10. The four intermetallic phases were generated during diffusion process. The generalized Wagner method was proposed for determination of intrinsic diffusion coefficient and the entropy production was calculated. The entropy production allowed for determination of the sequence of phase growth [22].

Experimental

The rods of CuNi (high purity model alloys) with nominal compositions of samples 1–6: 10 at.%Ni + 90 at% Cu, 30 at.%Ni + 70 at% Cu, 40 at.%Ni + 60 at% Cu, 60 at.%Ni + 40

***Corresponding author: Bartek Wierzba,** Rzeszow University of Technology, al. Powstańców Warszawy 12, 35-959 Rzeszów, Poland, E-mail: bwierzba@prz.edu.pl
Wojciech J. Nowak: E-mail: w.nowak@prz.edu.pl, **Daria Serafin:** E-mail: darseraf@gmail.com, Rzeszow University of Technology, al. Powstańców Warszawy 12, 35-959 Rzeszów, Poland

at% Cu, 70 at.%Ni + 30 at% Cu and 90 at.%Ni + 10 at% Cu, respectively were produced by Goodfellow in England. Then, the thick discs were cut from the ingot by spark erosion. The surfaces of the discs were ground and polished to mirror finish using SiC papers and diamond pastes down to 0.25 μm particle size. The high purity Ti discs were also cut from rod and polished with the same accuracy. Such prepared discs were connected in molybdenum holder to form the diffusion couple. The specimens were annealed in tube furnace in protective argon atmosphere at the temperature of 1,123 K for 160 hours. After annealing, the discs were cut in two halves and metallographic cross-sections were ground and polished. No Kirkendall-Frenkel effect was observed in the microphotographs. The samples were then analyzed by the EDS in the SEM to obtain the concentration profiles in the bulk interdiffusion zone. The concentration profiles allowed for determination of the diffusion paths in the isothermal ternary phase diagram.

Results

Figures 1, 2, 3, 4, 5 and 6 show the microphotographs of cross-sections of diffusion couples with the description of the formed intermetallic phases. Moreover, the pictures (on the right hand side) present the diffusion paths on the isothermal ternary phase diagram. The dots represent the concentration of the components – Ti, Ni and Cu. Qualitatively, the initial concentration of Cu and Ni determines the diffusion path and formed intermetallic phases. Moreover, after diffusion of sample 1 (Ti-Ni10Cu90) and 2 (Ti-Ni30Cu70) the two-phase zones were generated between the base material and τ_1 (Ti(Ni$_x$Cu$_{1-x}$)$_2$) phase. The generation of two-phase zone determines that the diffusion crosses the tie lines (conodes) during the diffusion process. In the rest samples the two-phase zone is not observed.

The slight increase of Ni concentration in base material – 30 at% causes the completely different relaxation

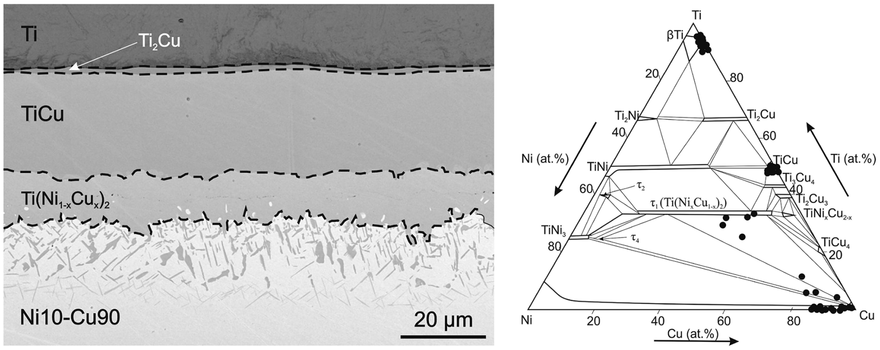

Figure 1: Left – the microphotography showing grown intermetallic phases, right – the diffusion path in diffusion couple experiment Ti-Ni10Cu90 at 1,123 K after 160 h.

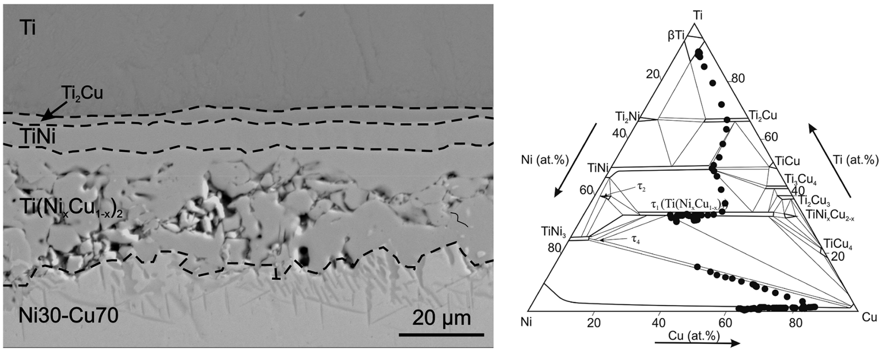

Figure 2: Left – the microphotography showing grown intermetallic phases, right – the diffusion path in diffusion couple experiment Ti-Ni30Cu70 at 1,123 K after 160 h.

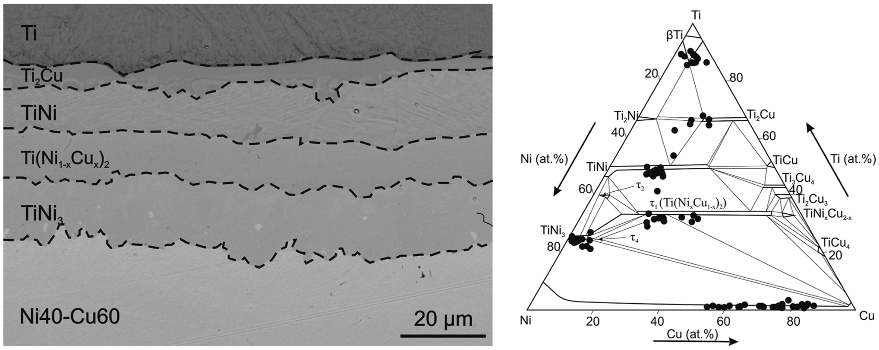

Figure 3: Left – the microphotography showing grown intermetallic phases, right – the diffusion path in diffusion couple experiment Ti-Ni40Cu60 at 1,123 K after 160 h.

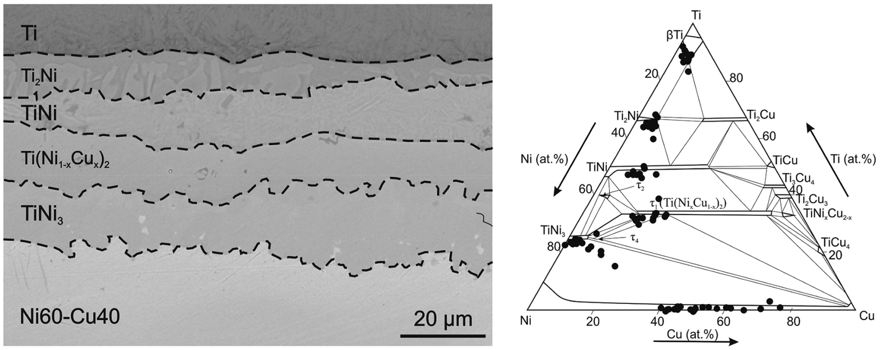

Figure 4: Left – the microphotography showing grown intermetallic phases, right – the diffusion path in diffusion couple experiment Ti-Ni60Cu40 at 1,123 K after 160 h.

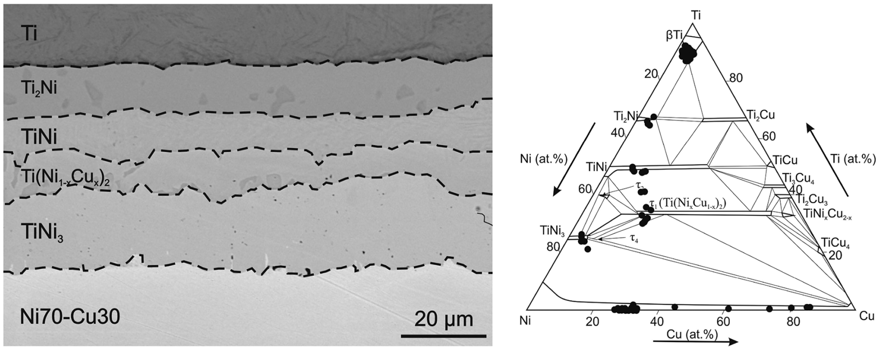

Figure 5: Left – the microphotography showing grown intermetallic phases, right – the diffusion path in diffusion couple experiment Ti-Ni70Cu30 at 1,123 K after 160 h.

during the diffusion process. In sample1, the following phases will be generated during the diffusion process: $Ni_{10}Cu_{90}$ → $Ni_{10}Cu_{90} + τ_1$ ($Ti(Ni_xCu_{1-x})_2$) →uTiCu → Ti_2Cu →uTi. However, the diffusion path in sample 2 is different: $Ni_{30}Cu_{70}$ → $Ni_{30}Cu_{70} + τ_4$ ($TiNi_3$) → $τ_1$ ($Ti(Ni_xCu_{1-x})_2$) →-TiNi → Ti_2Cu →uTi. The qualitative analysis shows that different two-phase zones are formed, namely$Ni_{10}Cu_{90} + τ_1$ ($Ti(Ni_xCu_{1-x})_2$) and $Ni_{30}Cu_{70} + τ_4$ ($TiNi_3$), moreover during diffusion in sample1 the TiCu phase will be generated and in sample 2 – TiNi phase. These differences depend

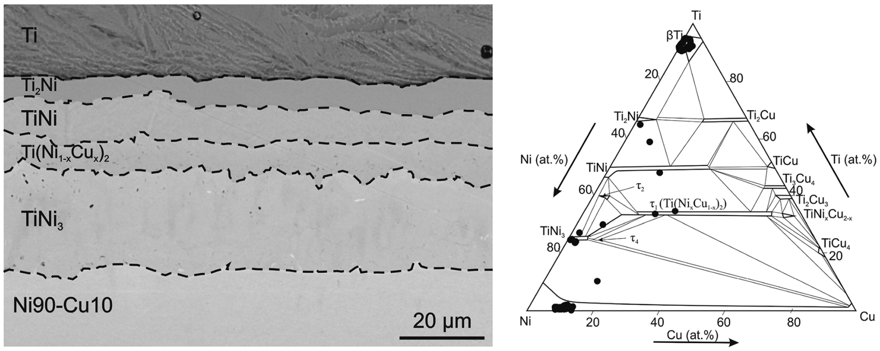

Figure 6: Left – the microphotography showing grown intermetallic phases, right – the diffusion path in diffusion couple experiment Ti-Ni90Cu10 at 1,123 K after 160 h.

on the initial concentration of Ni in base material. The τ_4 phase is not seen in the microphotography – Figure 2. The most probable reason is that this phase is consumed during the diffusion because of its low diffusion coefficients are low.

The dissimilarity can be seen also in the thickness of the intermetallic phases, namely with increasing of Ni content the volume of Ti_2Cu phase decreases. However, the τ_1 phase behaves in the opposite way. This anomalous can be explained by the difference in diffusion coefficients and thermodynamic data in TiNi and TiCu phases.

When the content of the Ni is more than 40 at% the two-phase zone is not generated, thus the diffusion goes through the tie-line – the phases are in thermodynamic equilibrium. However, the diffusion paths are different. In case of sample3 – Ti-Ni40Cu60 the diffusion goes through: Ti-Ni40Cu60 → τ_4 ($TiNi_3$) → τ_1 ($Ti(Ni_xCu_{1-x})_2$) →-TiNi → Ti_2Cu iNTi. The diffusion path with Ni content greater than 60 at% goes through the Ti_2Ni phase instead of Ti_2Cu.

The qualitative difference can also be observed in thicknesses of each phase. For example $TiNi_3$ is thicker with increasing of Ni content – Figures 4, 5 and 6.

The relaxation path for diffusion process, when more than one diffusion path is possible is still an open problem in diffusion community. The hypothesis is that the diffusion path with the greatest value of entropy production will be chosen. In fact the entropy production is baricentric average of the square of diffusion fluxes. However, in determination of diffusion velocity is very important task. In case of multiphase ternary diffusion couple diffusion coefficients can be determined from the kinetic process and more accurate modified Wagner method.

In case of one phase growth, for example oxidation process, the growth of the phase can be determined form parabolic rate law:

$$\frac{dX}{dt} = \frac{k(t)}{X(t)} \tag{1}$$

where $X(t)$ is the thickness of the product layer and $k(t)$ the instantaneous rate constant.

$$k(t) = \frac{1}{RT} \int_{\mu''_A}^{\mu'_A} D_A^{ox} d\mu_A^{ox} \tag{2}$$

where μ'_A and μ''_A are chemical potentials at the left and right side of the oxide phase, D_A^{ox} denotes the diffusion coefficient of oxidized element in oxide phase.

Thus, the diffusion coefficient can be calculated from eq. (2). In case of more complicated systems, where more than one reaction layer occurs, the Wagner method should be used in determination of the integral diffusion coefficient. The final equation for intrinsic diffusion coefficient in multiphase system can be written as follows:

$$\begin{aligned}\int_{N_k^{(i)\prime}}^{N_k^{(i)\prime\prime}} D dN_k = {} & \frac{\left(N_k^{(i)} - N_k^-\right)\left(N_k^+ - N_k^{(i)}\right)}{N_k^+ - N_k^-} \times \left[\frac{\left(\Delta x^{(i)}\right)^2}{2t}\right] + \\ & + \frac{\Delta x^{(i)}}{2t}\left[\frac{N_k^+ - N_k^{(i)}}{N_k^+ - N_k^-} \times \int_{-\infty}^{x^{(i-1,i)}} \frac{\Omega_m^{(i)}}{\Omega_m}\left(N_k - N_k^-\right)dx \right. \\ & \left. + \frac{N_k^{(i)} - N_k^-}{N_k^+ - N_k^-} \int_{x^{(i,i-1)}}^{\infty} \frac{\Omega_m^{(i)}}{\Omega_m}\left(N_k^+ - N_k\right)dx\right]\end{aligned} \tag{3}$$

where: upper indexes denote the phase, N_B^- and N_B^+ are the initial mol fractions at the end of the diffusion couple, $\Delta x^{(i)}$ is the thickness of the generated phase after time t, and $\Omega_m^{(i)}$ denotes the molar volume. The diffusion coefficient is calculated from known phase thickness and molar concentrations in base materials and at the boundaries of each phase. Thus the experimental profiles should be known. The Wagner diffusion coefficient is an effective diffusivity. In case of multiphase systems this coefficient depends on the neighboring phases, thus in each sample this kinetic constant can be different. The results obtained for sample 3 in each phase is presented in Table 2. In Table 1. the diffusion coefficients for pure Ti [24], Ni [25] and Cu [26] are presented.

Table 1: The diffusion coefficient of pure Cu, Ni and Ti.

Component	Diffusion coefficient, cm^2s^{-1}
Ni	$D_{Ni}^{Ni} = 1.24 \cdot 10^{-13}$
Cu	$D_{Cu}^{Cu} = 1.33 \cdot 10^{-10}$
Ti	$D_{Ti}^{Ti} = 1.09 \cdot 10^{-13}$

When the kinetic parameters are known, the phase competition – the sequence of phase formation, can be determined. The hypothesis is that the first phase will appear characterized with the biggest entropy production, eq. (4) [22].

$$\sigma = -\frac{1}{T}\sum_{k=1}^{n} J_k \ \mathrm{grad}\mu_k \tag{4}$$

where σ denotes the entropy production, J_k the diffusion flux and μ_k chemical potential. Equation (4) in fact is a baricentric average of the diffusion fluxes. The hypothesis of the maximum entropy production and first phase growth can be simply checked in binary systems, where the maximal diffusion flux determines the sequence of phase growth [21]. In ternary system this problem is much more complicated. However, the maximum of entropy production is related with to the maximum of square of diffusion flux. The maximum of the diffusion flux sets the major trend of diffusion, thus the diffusion follows the maximum of the flux. The equation of entropy production can also be written as optimization problem by a norm notation as follows:

$$\sigma = -\frac{1}{T}\sum_{i=1}^{r}\frac{J_i^2}{B_i c_i} \approx \omega\left\|\frac{N^{eq}-N}{\kappa}\right\| \tag{5}$$

where ω and κ are weight functions. N^{eq} and N are the composition vectors for time t and in thermodynamic equilibrium.

Similar like Wagner method eq. (4) cannot be directly used in calculations of entropy production in a system characterized with low non-stoichiometry – gradient of concentration is almost zero. Thus, the gradient operator should be ejected from the right side of the equation. Assuming, that the chemical potential can be calculated from the Gibbs energy:

$$\mu_i^{(v)} = \partial g^{(v)} / \partial c_i^{(v)} \tag{6}$$

where $g^{(v)}$ denotes the Gibbs energy in (v) phase. The entropy production can be discretized as follows:

$$\begin{aligned}\bar{\sigma}^{(v)} = \frac{1}{T}\sum_{i=1}^{r} c_i^{(v)} B_i^{(v)} &\left|\frac{g^{(v+1)}-g^{(v)}}{c_i^{(v+1)}-c_i^{(v)}} - \frac{g^{(v)}-g^{(v-1)}}{c_i^{(v)}-c_i^{(v-1)}}\right| \\ &\left|\frac{g^{(v+1)}-g^{(v)}}{c_i^{(v+1)}-c_i^{(v)}} - \frac{g^{(v)}-g^{(v-1)}}{c_i^{(v)}-c_i^{(v-1)}}\right|\end{aligned} \tag{7}$$

where $\bar{\sigma}^{(v)}$ denotes the local entropy production, $\bar{\sigma}^{(v)} = \sigma^{(v)}(\Delta x)^2$. Equation (7) allows for determination of the entropy production in each phase in the ternary and higher systems. Please note, that the entropy production in (v) phase depends on the Gibbs energy in neighboring phases.

The calculated Wagner's diffusion coefficients as well as the entropy production can be approximated with the calculation error. The mean concentration of the components in intermetallic phases was used in the calculations. Such assumption could increase the numerical error of the

Table 2: The average Wagners integral diffusion coefficient calculated from eq. (3).

Average Wagners integral diffusion coefficient, cm^2s^{-1}			
Phase	Ni	Cu	Ti
τ_4 ($TiNi_3$)	$D_{Ni}^{\tau_4} = 1.42 \cdot 10^{-12}$	$D_{Cu}^{\tau_4} = 5.25 \cdot 10^{-13}$	$D_{Ti}^{\tau_4} = 7.17 \cdot 10^{-13}$
τ_1 ($Ti(Ni_xCu_{1-x})_2$)	$D_{Ni}^{\tau_1} = 2.57 \cdot 10^{-13}$	$D_{Cu}^{\tau_1} = 5.44 \cdot 10^{-13}$	$D_{Ti}^{\tau_1} = 6.30 \cdot 10^{-13}$
TiNi	$D_{Ni}^{TiNi} = 1.89 \cdot 10^{-13}$	$D_{Cu}^{TiNi} = 4.05 \cdot 10^{-13}$	$D_{Ti}^{TiNi} = 6.82 \cdot 10^{-13}$
Ti_2Cu	$D_{Ni}^{Ti_2Cu} = 1.39 \cdot 10^{-14}$	$D_{Cu}^{Ti_2Cu} = 2.18 \cdot 10^{-13}$	$D_{Ti}^{Ti_2Cu} = 1.91 \cdot 10^{-13}$

model. Moreover, the analysis of the experimental results shows, that both Wagner's diffusion coefficient as well as entropy production depend on the initial composition of the diffusion pair. Nevertheless, the results of the entropy production in a proper way determine the competition in the binary systems, Table 3. To minimize the possible errors of derivation, the backward and forward differences of chemical potential over the phase *(v)* have been applied.

Table 3: The entropy production in Ti-NiCu system, sample 3.

Phase	Entropy production
T_4 ($TiNi_3$)	$\bar{\sigma}^{\tau_4} = 5.64 \cdot 10^{-31}$
T_1 ($Ti(Ni_xCu_{1-x})_2$)	$\bar{\sigma}^{\tau_1} = 5.88 \cdot 10^{-31}$
TiNi	$\bar{\sigma}^{TiNi} = 2.40 \cdot 10^{-31}$
Ti_2Cu	$\bar{\sigma}^{Ti_2Cu} = 1.19 \cdot 10^{-31}$

Figure 7 shows the values of the entropy production in sample 3. It can be seen, that the prediction is that the τ_1 ($Ti(Ni_xCu_{1-x})_2$) will grow as first after that the τ_4 ($TiNi_3$) will appear next will be the TiNi and as the last Ti_2Cu will form.

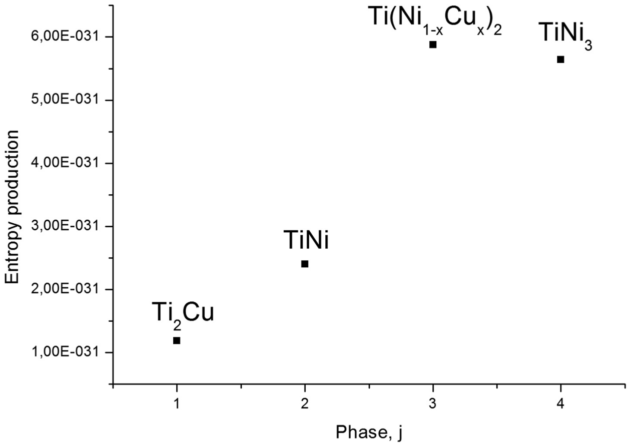

Figure 7: The graph showing calculated entropy production in sample 3 for four generated phases.

The calculations strictly depend on kinetic and thermodynamic data, thus the method can be used as first approximation of the competition problem. However, the hypothesis of the maximum of entropy production can be applied to much more similar problems like: approximation of the intersection point of the diffusion path with the phase boundary [1], the uniqueness determination of the diffusion path during the diffusion process [22].

Conclusions

In the present paper the diffusion in Ni–Cu–Ti system was analyzed. Six different diffusion couples were prepared with different amount of Ni and Cu and then coupled with pure Ti. The Wagner method was used for calculation of the integral diffusion coefficients in each phase. Moreover, the kinetic and thermodynamic parameters were then introduced in calculations of entropy production. The maximization of the entropy production allowed for determination of the phase growth order during diffusion process. The method can be further generalized to calculate the kinetic of the diffusion reaction processes in multiphase systems, e. g. internal oxidation process in NiPtO alloy.

Acknowledgements: This work was supported by the National Science Centre (NCN) in Poland, decision number 2014/15/B/ST8/00120.

References

[1] B. Wierzba, High Temp. Mater. Proc., 36 (2017) 447.
[2] Z. Grzesik, M. Migdalska and S. Mrowec, High Temp. Mater. Proc., 29 (2010) 203.
[3] C. Matano, Jpn. J. Phys., 8 (1933) 109.
[4] B. Wierzba and W. Skibiński, J. Alloys Compd., 687 (2016) 104e108.
[5] B. Wierzba and W. Skibiński, Phys. A, 392 (2013) 4316.
[6] B. Wierzba and W. Skibiński, Phys. A, 440 (2015) 100.
[7] C. Wagner, Acta Metallurgica., 17 (1969) 99.
[8] W.J. Boettinger, J.A. Warren, C. Beckermann and A. Karma, Ann. Rev. Mater. Res., 23 (2002) 163.
[9] L.Q. Chen, Ann. Rev. Mater. Res., 32 (2002) 113.
[10] L.Q. Chen and W. Yang, Phys. Rev. B, 50 (1994) 15752.
[11] S. Hu and L. Chen, Acta Mater., 49 (2001) 463.
[12] D. Rodney, Y. LeBouar and A. Finel, Acta Mater., 51 (2003) 17.
[13] Y.U. Wang, Y.M. Jin, A.M. Cuitino and A.G. Khachaturyan, Appl. Phys. Lett., 78 (2001) 2324.
[14] Y. Jin, Y. Wang and A. Khachaturyan, Appl. Phys. Lett., 29 (2001) 3071.
[15] H. Henry and H. Levine, Phys. Rev. Lett., 93 (2004) 105504.
[16] D. Bhate, A. Kumar and A. Bower, J. Appl. Phys., 87 (2000) 1712.

[17] A. Kazaryan, Y. Wang and B. Patton, Scripta Mater., 41 (1999) 487.
[18] X. Jing, J. Zhao, G. Subhash and X.-L. Gao, Mater. Sci. Eng. A, 412 (2005) 271.
[19] Y. Wang, Acta Mater., 54 (2006) 953.
[20] Q. Du, C. Liu and X. Wang, J. Comput. Phys., 212 (2006) 757.
[21] T. Biben, K. Kassner and C. Misbah, Phys. Rev. E, 72 (2005) 041921.
[22] M. Danielewski, B. Wierzba, A. Gusak, M. Pawełkiewicz and J. Janczak-Rusch, J. Appl. Phys., 110 (2011) 123705.
[23] B. Wierzba, Physica. A, 454 (2016) 110.
[24] M. Koppers, C. Herzig, M. Friesel and Y. Mishin, Acta Mater., 45 (1997) 4181.
[25] R.E. Hoffman, F.W. Pikus and R.A. Ward, Trans. AIME, 206 (1956) 483.
[26] A. Kuper, H. Letaw, L. Slifkin, E. Sonder and C.T. Tomizuka, Phys. Rev., 96 (1954) 1224.